Performance Evaluation of Improved Flexible Runway Pavement under Aircraft Loads

*Saima Ali[1], Xuemei Liu[2], David Thambiratnam[3], and Sabrina Fawzia[4]

[1] Research Fellow, School of Civil Engineering and Built Environment, Queensland University of Technology

[2] Senior Lecturer, Department of Infrastructure Engineering, The University of Melbourne

[3] Professor, School of Civil Engineering and Built Environment, Queensland University of Technology

[4] Senior Lecturer, School of Civil Engineering and Built Environment, Queensland University of Technology

*Corresponding Author- email address: saima.ali@qut.edu.au, shoma2011@gmail.com, contact number: +61405587365

Abstract

Safe runway pavements are essential for the smooth landing of aircraft. Due to aircraft movements, these pavements are subjected to large dynamic loads which can cause their failure and jeopardise safety. This paper proposes the use of improved cement-based layers to enhance the performance of flexible runway pavements. The performance of such retrofitted runway pavements under both static and moving loads is investigated by experimental study and three dimensional numerical simulations. Results indicate that the improved cement-based layers can significantly reduce surface deflections in the runways under heavy static and moving loads. Under heavy moving loads, the proposed cement-based layers can distribute the vertical stresses to the surrounding soil area, significantly reduce surface deformations and prevent failure. Findings of this research will contribute towards improved designs of runway pavements resulting in enhanced safety and failure mitigation.

1. Introduction

Modern runway pavement systems accommodate heavy and large aircrafts and such pavement systems are often subjected to high speed moving loads during taking off and landing of aircrafts. The slow movement of aircraft also imposes static compression on the runway pavements [1]. Recently, many very heavy aircraft have been introduced to fulfil travel demands. These aircraft impose large compressive strains or vertical deflections on the surface layer of flexible runway pavements composed of dense graded asphalt [2] adjacent to the wheel regions. Current runway systems have not been adequately evaluated under increased loading conditions. Their performance under heavy dynamic loading needs to be enhanced to avoid pavement failure and jeopardise aircraft safety.

According to the AC 139.C07 v.10 [3], a standard flexible runway pavement of Australia consists of Hot Mix Asphalt (HMA), base layer, sub-base layer and subgrade layer, as shown in Figure 1. The surface layer is composed of densely graded HMA with thickness of 40–60 mm [3, 4, 5, 6]. The base and sub-base layers are usually composed of crushed rock or gravel as unbound base or sub-base course. Cement or lime-stabilised base and sub-base course is used in practice [3]. The base thickness can be approximately 150 mm or larger, whereas the sub-base thickness can be less than the base layer thickness [3, 4, 5, 6]. These layers then rest on a natural subgrade to disperse the load uniformly. Woo et al. [7] reported that stiff interlayers (base and sub-base) could play significant role in improving the load bearing capacity of a multi-layer composite structure such as a flexible runway. Hence, further research is necessary to explore appropriate rigid materials for the base and sub-base layers of runway pavement and evaluate the performance of the structure in reducing surface damage to the runway.

Many studies have been conducted using laboratory, field or finite element (FE) modelling methods to investigate the response of runway pavements under different loading conditions. Some researchers investigated the performance of flexible pavements under moving loads. Kim and Tutumluer [8] conducted a FE study on effects of moving aircraft load on pavement runway to predict the magnitude and direction of deflections at the surface layer and subgrade under tandem and tridem axle pavement conditions. The results show that proper characterisation of pavement foundation geomaterials (subgrade soil and base and sub-base layers) significantly affects the critical response of pavement. Su et al. [9] investigated the significance of using recycled asphalt concrete on the surface layer of airport runway pavement through a full scale laboratory experiment with wheel tracking test. Su et al. [9] found that the recycled asphalt concrete is effective in reducing the initial deflection compared to that of the normal asphalt concrete. However, Su et al. [9] found from FE analysis that the long-term performance of both types of asphalt concrete was similar. Few researchers [10, 11, 12, 13] investigated the performance of runway under dynamic loadings including hard landing and impact loads through rigorous in-situ test and FE analysis and determined the deflection, stress, and strain. Al-Qadi et al. [14] conducted rigorous in situ test at the Cagliari-Elmas airport in Italy to investigate the stresses and strains of flexible runway pavement under aircraft loading. Kuo et al. [10] investigated the effect of inclined impact loading on runway pavement caused by hard landings of heavy aircraft. Kuo et al. [10] inferred that when there is impact on runway pavement at an angle of 0.2–0.8° above the horizontal, the impact load remains equal to the static load imposed by the aircraft such that impact angles above 0.8° result in fatigue cracking and permanent deformation of airport pavement, and the

damage on the pavement increases with the increase in the landing angle. In addition, Kuo et al. [10] also observed the amplification of tensile strains and compressive strain at the base of the asphalt layer and at the top of the subgrade when impact loading is taken into considered rather than static loading.

As reported in the literature, different loading conditions were selected to investigate the performance of existing runway pavement with unbound base layer. However, there has not been any significant research to improve the performance of flexible runway pavement in terms of deflection under aircraft loading. Hence, there is a need for research and detailed parametric study to understand the behaviour of flexible runway pavement under static and moving loads and to investigate efficient methods to improve the performance under these loading conditions.

A flexible runway pavement can be considered as a cement-based multi-layer composite structure comprised of multiple layers with the major function conducted by the united action of the sacrificial layer and the core. The top surface layer and the interlayer are considered as the sacrificial layer and core layer, respectively. Numerous experimental and numerical studies have been carried out to explore the behavior of multi-layer composite metal structures [7,15,16,17,18,19,20,21,22,23,24,25,26,27]. These researchers inferred that the purpose of the sacrificial layer is to protect the core from the initial load intensity. It implies that the top surface layer of the composite structure acts as the sacrificial layer to absorb the initial energy coming from the dynamic loads. The core portion (below the surface layer) of the multi-layer composite structure usually absorbs a reduced amount of impact energy compared to the sacrificial layer (upper-most layer) and the bottom layers absorb the least amount of energy developed from the dynamic loads [7].

The current study followed the concept of multi-layer composite and suggested suitable materials in the different layers to enhance the performance of flexible runway pavement. Performance of two different types of proposed (Type 1 and Type 2) (Table 1) flexible runway pavements are evaluated and are compared with that of a conventional flexible runway under static loading. Type 1 flexible runway pavement used high strength concrete in the base layer and cement treated aggregate in the sub-base layer. Type 2 flexible runway pavement used high strength concrete in the base layer and cement mortar in the sub-base layer. A three-Dimensional (3D) FE model of the conventional runway pavement is established and validated using test results. The comparative study enabled to identify a feasible composition of the flexible runway pavement. The aim of the study was then determined under dynamic loads from heavy aircraft. Results indicated enhanced performance by using proposed flexible runway pavements with less likelihood of failure under credible loads.

2. Experimental Investigation

In this study, typical category of flexible runway specimen used in Australia [3] was tested under static loading to investigate its static behaviour. The test results were also used to validate the FE model used in the numerical analysis.

2.1 Specimens and materials

A conventional flexible runway specimen with two layers was prepared according to Australia standards [3]. The surface layer was composed of densely graded asphalt concrete, whereas the base and sub-base layers were composed of cement-treated

aggregate (Figure 2). Dimensions of the specimen were 1 m × 1m with a total depth of 350 mm. The thickness of the asphalt concrete layer was 85 mm and the total depth of the cement-treated aggregate layer was 265 mm. Two galvanised steel hollow tubes, which were used for lifting the specimen, were fitted into the specimen before casting. The tubes were placed with a vertical clear cover of 75 mm from the base of the specimen (Figure 2).

The modulus of elasticity, Poisson's ratio and compressive strength of the cement-treated aggregate in the base and sub-base layers of the specimen were determined from standard cylindrical tests according to AS1012.2:2014 [28]. Five cylindrical specimens of each layer with dimensions of Ø100 x 200 mm were prepared and tested   under a loading rate of 1 mm/min and at a temperature of 25^0 C following the same standard [28]. The tensile strength of the cement-treated aggregate was measured according to ASTM C78/78M [29]. The loading rate for the flexural test was also maintained at 1 mm/min and the load–deflection curve was recorded at the mid-span. Results from the testing are presented in Table 2.

2.2 Test Procedure

The compressive tests were conducted using a hydraulic compressive testing machine with the specimens placed directly on a strong floor to avoid global vertical deflection of the specimen. Figure 3 shows the test set-up of specimens and instrumentation. A 45-mm thick load bearing plate with a diameter of 200 mm was used for loading at the centre of each specimen. The test was a pure compression test as vertical deflection was not allowed at the base of the composite specimen by supporting the composite specimen through strong floor. The static compressive test was carried out following the Chinese Standard GB/T 50081-2002 [30]. The test was an unconfined compression test with the loading rate of 1 mm/min. Three linear variable differential transducers (LVDTs) were installed on the surface layer at three different locations in each specimen to measure the vertical deflection. The LVDTs were attached to a galvanised steel frame as shown in Figure 3(a). The compression testing machine was operated by hydraulic pressure with the applied loading rate of 1 mm/min.

2.3 Test results

The maximum load applied to the flexible runway specimen was 410 kN, taking into consideration the maximum loading capacity of the device. Vertical deflections on the top surface of asphalt concrete were recorded using the three LVDTs (Figure 3). No major cracks were observed around the periphery of the specimen. Figure 4 shows the deflection history curves of the flexible runway specimen under static compression.

Figure 4 shows that there is a gradual increase in the deflection at all three locations of the flexible specimen till about 150s after loading. Beyond this, there is a sharp increase in the deflections at A and B till about 600s, while the deflection at C increases at a reduced rate. It occurred because the locations A and B are at two opposite sides of the top surface centre of the specimen and relatively closed to the centre of the specimen compared to the location C.

From 400 to 800s, the deflections increased by 56%, 47% and 33% at locations A, B and C respectively. The location A was closer to the top surface centre of the specimen compared to the location B and hence, higher rate of increase in deflection was found at location A compared to location B. Location C is at the corner of the top surface centre of the specimen and hence least rate in the increase of deflection was found. In the

4

last 250s of deflection history curves, similar sequence was noted at the selected locations leading to a final deflection at A, B and C around 1.7 mm, 1.65 mm and 1.35 mm, respectively at the loading time of 1122s and load of 410 kN. The hydraulic compressive testing machine was able to apply maximum load of 410 kN within 1122 seconds. So, the test was not further continued.

The static compression test results on the flexible runway specimen show that as the compressive loads increase, downward vertical deflections of the top asphalt concrete surface significantly increase up to a certain period; thereafter, the effect of the applied load becomes less significant. This is possibly due to the better settlement capability of the asphalt layer under the applied compressive load.

2.4 Finite element modelling

A 3D nonlinear FE model was developed using ABAQUS/Explicit to simulate a flexible runway subjected to gradual compressive loads and moving loads.

2.4.1 Element selection and material modelling

The FE model had three different parts representing the asphalt concrete layer, the cement-treated aggregate layer and the two hollow galvanised steel tubes. The influence of the galvanised steel tubes on the results was negligible and hence this was ignored. The asphalt concrete layer and the cement-treated aggregate layer were modelled using 8-node linear brick elements with reduced integration and hourglass control (C3D8R). Asphalt concrete was modelled using a linear viscoelastic model by defining Prony series values at 25 °C. The cement-treated aggregates were considered as concrete-like materials and defined using a concrete damage plasticity model. Compressive and tensile stress–strain curves obtained by following a procedure similar to that in Ali et al. [31] were used to define the corresponding strength properties of tested cement-treated aggregate. Material properties used in the FE model are listed in Table 2.

a) Prony-series type viscoelastic model

A generalization of Maxwell model including several Maxwell branches in parallel can be used to better predict the material behavior as well as describe a wider range of viscoelastic materials [32].

In this generalized model, the total strain ε, is identical in all branches while the total stress is the sum of stresses in the n + 1 branches of the model. In three dimensions, the effective stress $\tilde{\sigma}$ can be formulated in terms of the total strain ε, and the deviatoric strain rate $\dot{e}$ as described in equation (1). According to experimental observations, material viscous behavior is found to be driven by changes in shape [42] [33], while the changes in volume are observed to be elastic. Thus, as shown in equation (1), the bulk modulus, K, is time independent while only the deviatoric stress is written in the form of a convolution integral.

$$\tilde{\sigma}(t) = \tilde{\sigma} \text{vol} + \tilde{\sigma} \text{dev}(t) = Ktr(\varepsilon)I + 2 \int_{-\infty}^{t} G(t-\tau)\dot{e}(\tau)d\tau \qquad (1)$$

where tr(·) is the trace operator, I is the identity tensor and ε the total strain tensor. The elastic bulk modulus, K and shear modulus, G are related to the Young's modulus, E and Poisson ratio, ν by G = E 2(1+ν) and K = E 3(1−2ν).

The material modulus, G(t) which represent the shear relaxation modulus is given in the Prony-series form of equation (2).

$$G(t) = G\infty + n \sum i=1 \text{ } Gi\exp(−t/\lambda i) = G0 \text{ } \mu\infty + n \sum i=1 \text{ } \mu i\exp(−t/\lambda i) \qquad (2)$$

As described in [42], the parameters μ in the series are the normalized relaxation modulus in which, μ∞ = G∞ G0 , μi = Gi G0 and G0 is the instantaneous shear modulus at time zero.

ABAQUS can calculate the Prony series terms mentioned above from the specified creep test data. The creep test data mentioned by Modarres and Shabani [34] is used for the model validation as the literature and the present research work used both used dense graded asphalt concrete.

b) Concrete damage plasticity model

"Concrete Damage Plasticity Model" is used to define the plasticity parameter and the non-linear behavior of material under uniaxial tension and uniaxial compression. "Concrete Damage Plasticity Model" (CDP) available in ABAQUS software is a modification of Drucker-Prager strength hypothesis which considers that the failure surface in the deviatoric cross section is not required to be a circle and it is governed by parameter K_c (Kmiecik and Kaminski, 2011) [35]. The default value of K_c in ABAQUS is 0.67. Besides, in the CDP model the plastic potential surface in the meridional plane assumes the form of a hyperbola.

The shape is adjusted with eccentricity which is a small positive value that expresses the rate of approach of the plastic potential hyperbola to its asymptote (Kmiecik and Kaminski, 2011)[35]. The *eccentricity* can be calculated as the ratio of tensile strength to compressive strength (Jankowiak et al., 2005)[36]. The default value of eccentricity, *e* in ABAQUS is 0.1. Another parameter used in the CDP is f_{b0}/f_{c0}, the ratio of initial equibiaxial compressive yield stress to initial uniaxial compressive yield stress. The default value of this ratio in ABAQUS is 1.16. Another parameter in CDP model is *Dilation Angle*, ψ which is the angle of inclination of the failure surface towards the hydrostatic axis, measure in the meridional plane. *Dilation Angle* of concrete like materials can be considered as internal friction angle (Kmiecik and Kaminski, 2011) [35]. Compressive stress data can be provided as a tabular function of inelastic (or crushing) strain. Tensile stress data can be provided as a tabular function of inelastic (or cracking) strain or by displacement data or fracture energy data. The relevant figures and information are mentioned in Ali et al. [37].

Mesh convergence analysis was first performed to ensure that the FE model can provide accurate results and mesh sizes of 10 mm and 5 mm were adopted for the cement-treated aggregate and asphalt concrete, respectively. Tie constraints were defined between the cement-treated aggregate layer and asphalt concrete layer. The bottom of the runway specimen was modelled as pin-supported, whereas the sides had no constraints to simulate real test conditions. The resulting FE model is shown in Figure 5. It was analysed

under gradual compressive loads applied over the asphalt concrete surface as uniformly distributed pressure.

2.5 Model Validation

Deflections were monitored at three locations during the testing. Load deflection histories at these locations predicted by the FE model are compared with those obtained from the testing and the results are presented in Figure 6. It is evident that the two sets of deflection-time histories compare reasonably well. Deflections at locations A, B and C during the static compression test are 1.67 mm, 1.65 mm and 1.35 mm, respectively at the maximum load of 410 kN compared to 1.52 mm, 1.6 mm and 1.25 mm, respectively obtained from the FE analysis at the same locations and under the same load. Deviations of the FE results from the test results at locations A, B and C are 9%, 4% and 7.5%, respectively. These rather small deviations could be due to the less appropriate compaction of the asphalt concrete layer. In the FE model it was not possible to define the voids that were present in the asphalt concrete layer of the test specimen. Overall, results from the FE analysis and the experiment showed good agreement based on the trends of the FE and test curves and the percentage deviations of the maximum deflections.

3. Performance of the improved flexible runway pavement under gradual static loading

The geometries and materials used in the conventional flexible runway and the two proposed flexible runway pavement (Type 1 and Type 2) are presented in Table 1. Their performance is evaluated using the FE model and compared with that of a conventional flexible runway. Higher rigid materials with high elastic modulus were introduced in the proposed cement-based layers as such materials can efficiently counteract the dynamic loads acting on the structure [38]. Type 2 composition of the runway pavement was found to be effective by Ali et al. [39] in resisting impact loads compared to the Type 1 and conventional runway pavements.

The mechanical properties of the cement-treated aggregate, asphalt concrete and cement mortar were determined from laboratory tests, and the properties of high strength concrete were adopted from the study in Wu et al. [38]. The two pavement models were analysed under gradual compressive loads applied over the asphalt concrete surface as uniformly distributed pressure. The loading rate considered in the FE models was the same as that in the static test. Three locations were selected for investigation, as shown in Figure 7.

Figure 8 shows the load deflection curves of the pavement with different layers obtained from the feasibility study using FE analysis. The deflection curves at location A indicate that up to about 150 kN, both Type 1 and Type 2 flexible runway pavements with improved base layer behave similar to the conventional runway pavement, and the deflection is approximately 5 mm. When the load was increased to approximately 300 kN, the deflection of the conventional runway is 12% higher than those of the other specimens, and a similar trend is observed up to a load of 410 kN as shown in Figure 8(a). It is also evident that at location A, both Type 1 and Type 2 flexible runway pavements exhibit almost the same load deflection profiles across the entire loading regime. At location B, no significant differences in deflections were observed for all three types of

specimens up to a load of 50 kN. However, when the load reached approximately 200 kN, a significant increase (approximately 26%) is observed in the deflection of the conventional specimen compared to that of the proposed specimens. Significant deviations continued until a load of 410 kN, as shown in Figure 8(b). The performance of Type 1 and Type 2 specimens was very similar. On the other hand, the FE results at location C reveal that the deflections of the conventional specimen were significantly higher than those of the other two specimens at the initial stage of the loading. Deflections of Type 1 and Type 2 models remained the same up to about 100 kN, after which they deviate slightly, with Type 2 showing slightly better performance in reducing deflection at higher loads. At 410 kN, the deflections of Type 2 and Type 1 decreased by approximately 61% and 50%, respectively compared to that of the conventional runway. Deflection responses at location C in Figure 8(c) clearly show the superior performance of the two proposed flexible pavements compared to the conventional flexible pavement, with Type 2 showing a better performance than Type 1. Table 3 summarises the maximum deflections of the flexible runway specimens. These results demonstrate that surface deflections of runway pavements can be significantly reduced by using the proposed cement-based materials in the selected layers and enable enhanced performance of flexible runway pavements.

Type 2 specimen was found to be more efficient as the distance from the centre increases. Deflections at locations A, B and C can be decreased by 8%, 23% and 61% respectively compared to those of the standard flexible runway. Result of the feasibility study also shows that using a rigid base and sub-base instead of lighter material has significant effects on the reduction of surface deflections. Since asphalt concrete is expensive, concrete and mortar, which are easily available and cost effective, can be used for the base and sub-base to reduce deflection, instead of increasing the thickness of the asphalt concrete layer.

4. Performance of the improved flexible runway pavement under moving load

The developed FE model is used to investigate the performance of the improved flexible runway pavement under moving loads, after it is validated using the experimental results reported in Su et al. [9]. From the earlier section, Type 2 flexible pavement is more efficient (than the Type 1) in reducing the surface deflections in the asphalt concrete layer under gradual compressive loads. Therefore, a larger scale Type 2 pavement was further investigated to determine whether it can sustain moving aircraft loads.

4.1 Loading and model validation

The FE model was used to simulate the wheel tracking test conducted on an asphalt concrete sample with cross-section of 300 mm × 300 mm and height of 50 mm, as reported in Su et al. [9]. The specimen was subjected to back-and-forth movements of a rubber tyre with a contact pressure of approximately 1.38 MPa. Figure 9 shows an overview of the test setup of the wheel tracking test.

The contact area of the tyre and the top surface of the asphalt concrete sample were considered as rectangular and uniformly distributed loads corresponding to the above test were applied on the mentioned rectangular area [40]. Hence, the area of the uniformly distributed loads was considered equivalent to the load application area by the wheel [38] corresponding to the test of Su et al. [9]. To simulate the loading process, the wheel passing zone of asphalt concrete was divided into a few rectangular segments

(Figure 10) as contact areas of the tyre and the top surface of the asphalt concrete. In addition, several loading steps were defined to convey the simulation of wheel movement. In step 1, the wheel was over the first area from the left as shown in Figure 10. Hence, equivalent wheel load mentioned by Su et al. [9] was applied only over the first rectangular contact area (the first area from the left as shown in Figure 10) as uniformly distributed loads and loads over the next two rectangular area (Figure 10) was zero. Similarly, the wheel positioning and load application were simulated for the second area, third are and so on using different loading steps by providing uniformly distributed loads only over the area where the wheel stood with zero load on the other rectangular areas.

The asphalt concrete sample was tied up with the steel base layer using "Tie" constraint and the sides and bottom of both layers were provided with fixed supports to simulate the test conditions in Su et al. [9].

The rut depth after 100 passes of wheel over the asphalt concrete sample was recorded as 1 mm [9]. The FE analysis revealed that under similar test conditions, the vertical downward deflection after 100 passes of wheel was 0.94 mm, indicating a deviation of 6% from the test result. Therefore, the FE model can predict the behaviour of asphalt concrete surface under wheel loading, with reasonable accuracy.

4.2 Performance of proposed pavement under moving load

After validating the model using wheel tracking test, a larger scale Type 2 pavement was investigated to predict the behaviour of this runway pavement under moving load of Airbus 380. Moving load equivalent to aircraft take-off speed (90 m/s) was applied on the runway pavement and sub modelling of the runway pavement was considered to reduce the computation time. The area of the pavement model was selected as 20 m x 15 m since no change was observed in the maximum deflection beyond this area. The thicknesses of the layers are as mentioned in the previous section for Type 2 runway pavement model. The depth of the subgrade layer was selected as 2 m [39]. Figure 11 shows the FE model of the flexible runway with subgrade.

The material properties of asphalt concrete used in Modarres and Shabani [34] were adopted. Element selection and material modelling of the subgrade were carried out using the approach of Ali et al. [41]. Coarse mesh was selected for this large-scale flexible runway model, except for the asphalt concrete surface layer, to reduce the computation time. The mesh size of the subgrade layer was selected as 500 mm, whereas a mesh of 250 mm was selected for the cement mortar and high strength concrete layer. The mesh size for the asphalt concrete layer was selected as 100 mm and a mesh size of 50 mm was found appropriate for the loading zone of the asphalt concrete surface after performing mesh convergence analysis. Figures 11 and 12 show FE modelling of the runway pavement and the mesh convergence analysis at different loading steps, respectively. Fixed boundary conditions were applied at the bottom and sides of the proposed runway pavement.

Loading was applied from the front dual wheels of Airbus 380 over the top asphalt concrete surface using the approach described in the validated model under wheel tracking test in Su et al. [9]. The areas of the rectangles (0.6 m x 0.4 m) (shown in Figure 11) were subjected to moving load of uniformly distributed pressure of 726 kPa. The wheel contact area (0.24 m²) and the dimensions of the loading area (0.6 m x 0.4 m) were calculated using the approaches in Huang [40] and Leonardi [42], respectively.

The wheel pressure was calculated using half of the peak wheel acceleration given in Leonardi [43] since it was assumed that the acceleration of a moving wheel is reduced by 50% compared to the hard impact scenario of an aircraft. Three loading steps were defined for each rectangular area with smooth top amplitudes. The duration of each loading step was 0.04 s. The boundary conditions for the proposed flexible runway pavement were considered as pinned at sides of the pavement and fixed at the bottom of the pavement. Figures 13(a)–(c) show the observed deflection contours that help to evaluate the rut depths at the end of each loading step.

Maximum vertical deflections expressed in terms of rut depths on the top surface of the asphalt concrete layer under the wheel pressure of the moving aircraft were 1.54 mm, 1.07 mm and 0.74 mm corresponding to steps 1, 2, and 3, respectively. The three deflection contours reveal that the deflection (approximately 38% of peak deflection of the previous zone) from the previous loading surface remains after moving the wheel to the next loading zone. When the wheel remains in the last loading zone, approximately 26% deflection occurred compared to the first loading zone and the deflection in the first loading zone diminished as the wheel moves forward. This could be due to the flexible behaviour of asphalt concrete and this spreading phenomenon of deflection could be responsible for the reduction of peak deflection when the wheel moves forward.

Stress contours in Figures 14 (a)–(c) provide an idea of the shearing resistance of the proposed runway pavement. The maximum stresses occur at the top of the asphalt concrete surface of the runway model, and they were 8108 kPa, 4241 kPa and 3961 kPa corresponding to loading steps 1, 2, and 3, respectively. The three stress contours reveal that part of the stress of approximately 1060 kPa and 880 kPa remains on the first loading zone asphalt surface when the wheel pressure is only on the second and third loading zones, respectively. The peak stress reduces as the wheel move in forward direction on the adjacent area. These are favourable outcomes due to the proposed improved layers in the flexible runway pavement and will contribute towards its safety.

In addition, the established FE model predicted the fatigue behaviour of the proposed composite runway pavement under repeated moving loads. The process followed the approach of the wheel tracking test used to measure the performance of pavements. After repeated loading of 50 cycles, the maximum rut depth (Figure 15) was found to be almost similar to that in the first cycle. Since significant change in deformation was not found after 50 cycles, the improved runway pavement performs well under repeated moving loads from aircrafts. The shearing resistance of the proposed runway pavement under repetitive wheel loading was also found to be satisfactory as observed in Figure 16 as at 50 cycles, where the maximum stress was found to be almost similar to the maximum stress found at first cycle.

4.3 Parametric study under moving load

The parametric study was conducted to investigate the effects of a few key geometric and material parameters in controlling the rut depth of surface layer of Type 2 runway pavement under (large scale) under moving load of Airbus 380. These parameters include thickness of base and sub-base layer, compressive strength of base and sub-base layer and modulus of elasticity of asphalt concrete surface layer.

a) Effects of thickness of layers

The effects of the thickness of base and sub-base layers were studied on the Type 2 composite runway pavement under moving load of Airbus 380. The base thicknesses were selected as 165 mm, 265 mm and 365 mm and the sub-base thicknesses were selected as 100 mm, 200 mm and 300 mm. Figures 17 and 18 illustrate the variation of rut depth with the change of base and sub-base thickness at the three different loading steps described in previous section.

Figures 17 and 18 show that at all loading steps, the rut depths reduce with increase in base and sub-base thicknesses of the proposed multi-layer composite runway pavement. However, these variations are quite small and suggest that the standard base and sub-base thicknesses used in runway pavements in Australia are appropriate for the proposed multi-layer composite runway pavement.

b) Effects of compressive strength

The effects of compressive strength of base and sub-base layers of Type 2 multi-layer composite runway pavement in influencing the rut depth of the runway pavement were studied in this section. The compressive strengths for base layer were selected as 31 MPa, 54 MPa and 80 MPa whereas for the sub-base layer the strengths were 10 MPa, 20 MPa and 30 MPa.

Figures 19 and 20 show that at all loading steps, the rut depth reduces with increase in compressive strengths of base and sub-base layers of this proposed multi-layer composite runway pavement. These variations are however negligible within the selected ranges of the base and sub-base thicknesses and indicate that for the considered Airbus 380 (moving) load, normal strength concrete and normal strength mortar can be recommended for the base and sub-base layers respectively to reduce the rut depth.

c) Effects of modulus of elasticity of asphalt concrete

The effects modulus of elasticity of asphalt concrete surface layer on the rut depth of the Type 2 multi-layer composite runway pavement was studied. The selected moduli of elasticity of asphalt concrete were 6000 MPa, 7000 MPa and 8000 MPa.

Figure 21 shows that the rut depth of the proposed multi-layer composite runway pavement decreases significantly with the increase of modulus of elasticity of asphalt during all three loading steps. The reduction of deflection was found to be around 32% in each of the loading steps when the modulus of elasticity of asphalt concrete was increased from 6000 MPa to 8000 MPa. These results show that the use of asphalt concrete with higher modulus of elasticity can reduce the rut depth of the proposed multi-layer composite runway pavement under moving loads.

5. Conclusions

Safe runway pavements are essential for the smooth landing of aircraft. Due to aircraft movements, these pavements are subjected to large dynamic loads which can cause their failure and jeopardise safety. This paper proposes the use of improved cement-based layers to enhance the performance of flexible runway pavements. The performance of such retrofitted runway pavements under both static and moving loads is investigated using comprehensive experimental studies and three dimensional numerical simulations.

Two types of improved flexible runway pavement were investigated. The first type (Type 1) comprised of high strength concrete and cement treated aggregate in the base layer and sub-base layer respectively. The second type (Type 2) consisted of high strength concrete and cement mortar. The structural performances of the proposed flexible runway pavements were also compared to that of the conventional flexible runway pavement. Specific findings from this research are summarized below:

- The increase in vertical deflection was more significant for the conventional flexible runway pavement compared to the proposed flexible runway pavement with increase in the static compressive loads.
- The deflection was reduced by a significant amount (maximum 50%) when in the base layer, high strength concrete was used instead of cement treated aggregate and in the sub-base layer cement treated aggregate was used. Further the replacement of cement treated aggregate with cement mortar in the sub-base layer reduced the deflection around 61% compared to conventional runway pavement. The increase of the use of bound materials and consequently increasing the rigidity of the layers was found to effectively control the deflection of flexible runway pavements.
- The introduction of the rigid base and sub-base by using high strength concrete and cement mortar respectively enhanced the mechanical behaviour of flexible runway pavement under static compression and thereby the deflection was reduced.
- Under moving loads from heaviest aircraft, the flexible runway pavement with rigid base and sub-base (Type 2) is expected to distribute the vertical deflection and stress across the surrounding area instead of concentrating them and developing high deflection and stress in the loading area. Thus, minimal magnitude of rut depth and enhancement in shearing resistance under moving loading area can be realised.
- The fatigue behaviour of the proposed runway pavement is predicted to be satisfactory under repeated wheel loading
- Standard base and sub-base thicknesses used in the runway pavements in Australia can be considered for the proposed multi-layer composite runway pavement as there was insignificant change in rut depth within the selected range of thicknesses.
- Normal strength concrete and normal strength mortar can be recommended in the base and sub-base layer respectively to reduce the rut depth.
- Dense graded asphalt concrete with high elastic modulus is recommended for reducing the rut depth in the proposed runway pavement.

Results also indicated that the proposed flexible runway pavement has great potential to improve the performance of current runway pavements. Outcomes of the present study will contribute towards safer and more efficient performance of runway pavements.

REFERENCES

[1] G.A. Shafabakhsh, M. Motamedi, A. Family, Influence of asphalt concrete thickness on settlement of flexible pavements, Electronic Journal of Geotechnical Engineering 18 (2013) 473-483.

[2] M.C. Guercio, L.M. McCarthy, Y. Mehta, Mechanical properties and viscoelastic properties of asphalt mixtures under heavy static and dynamic aircraft loads, Transportation Research Board 2449 (1) (2014) 88-95.

[3] Strength Rating of Aerodrome Pavements, Advisory Circular of Civil Aviation Safety Authority, August 2011.

[4] G.W. White, An investigation on the Australian layered elastic tool for flexible aircraft pavement thickness design, Master of Engineering Thesis, University of New South Wales, 2007.

[5] L. Wardle, B. Rodway, Advanced design of flexible aircraft pavements, in: 24th ARRB conference 2010, Melbourne, Australia, 1-11.

[6] S. Ali, X. Liu, S. Fawzia, and D. Thambiratnam, Impact performance enhancement of runway pavement with improved composition, Journal of Engineering Failure Analysis 130 (2021) 1-11.

[7] S.C. Woo, J.T. Kim, J.Y. Kim, T.W. Kim, Impact energy and damage behaviour of hybrid composite structures under high velocity impact, in: 18th International conference on composite materials, 2011.

[8] M. Kim, E. Tutumluer, Multiple wheel load interaction in flexible pavements, Transportation Research Board 2068 (1) (2008) 49-60.

[9] Su, Y. Hachiya, R. Maekawa, Study on recycled asphalt concrete for use in surface course in airport pavement, Resources, Conservation and Recycling 54 (1) (2009) 37-44.

[10] S. Kuo, H. S. Mahgoub, R.D. Holliday, Pavement responses due to hard landing of heavy aircraft, Journal of the Transportation Research Board 1896 (2004) 88-95.

[11] H. Kim, W.G. Buttler. Finite element cohesive fracture modelling of airport pavements at low temperatures, Journal of cold regions science and technology, 57, (2009) 123-131.

[12] M. Bounsanti, G. Leonardi, A finite element model to evaluate airport flexible pavements response under impact, Journal of Applied Mechanics and Materials 138 (2011) 257-262.

[13] J. Wu. X. Liu, S.H. Chew, Parametric study on cement based soft-hard-soft (SHS) multi-layer composite pavement against blast load, Construction and Building Materials, 98 (2015) 602-619

[14] I.L. Al-Qadi, S. Portas, M. Coni, S. Lahouar, Runway instrumentation and response measurements, Journal of the transportation research board, 2153, (2010) 162-169.

[15] A. Othman, A. A. Arifin, S. Abdullah, A. K. Ariffin and N. A. N. Mohamed, Analysis of crushing laminated composite square tubes under quasi-static loading, Journal of Applied Mechanics and Materials, 446 (2013) 113-116.

13

[16] M. S. R. N. Kumar, M. M. M. Sarcar and V. B. K. Murthy, Static analysis of thick skew laminated composite plate with elliptical cutout, Indian Journal Engineering and Material Sciences, 16 (2009) 37-43.

[17] W. J. Cantwell and J. Morton, The impact resistance of composite materials-a review, Journal of composites, 22(5) (1991) 347-362.

[18] J. H. Park, S. K. Ha, K. W. Kang, C. W. Kim and H. S. Kim, Impact damage resistance of sandwich structure subjected to low velocity impact, Journal of Material Processing Technology, 201 (2008) 425-431.

[19] S. C. Her and Y. C. Liang, The finite element analysis of composite laminates and shell structures subjected to low velocity impact, Journal of Composite Structure, 66 (2004) 277-285.

[20] N. Jones, Inelastic response of structures due to large impact and blast loadings, Journal of Strain Analysis for Engineering Design, 70 (2010) 451-464.

[21] Z. Xue and J. W. Hutchinson, Preliminary assessment of sandwich plates subject to blast loads, International Journal of Mechanical Sciences, 45 (2003) 687-705.

[22] J. Yang and J. Li, An improved closed-form solution to interfacial stresses in plated beams using a two-stage approach. International Journal of Mechanical Sciences, 52 (2011) 13-31.

[23] Z. Kazanci and Z. Mecitoglu, Nonlinear dynamic behaviour of simply supported laminated composite plates subjected to blast load, Journal of Sound and Vibration, 317 (2008) 883-897.

[24] J. Xiong, A. Vaziri, L. Ma, J. Papadopoulos and L. Wu, Compression and impact testing of two layer composite pyramidal-core sandwich panels, Journal of Composite Structures, 94 (2012) 793-801.

[25] S. J. Salami, M. Sadighi, M. Shakeri and M. Moeinfar, An investigation on low velocity impact response of multilayer composite sandwich structures, Journal of Scientific world, article ID 175090 (2013).

[26] D. Karagiozova, G. N. Nurick, G. S. Langdon, S. C. K. Yuen, Y. Chi and S. Bartle, Response of asphalt sandwich-type panels to blast loading, Journal of Composite Science and Technology, 69 (2009) 754-763.

[27] H. Herranen, O. Pabut, M. Eerme, J. Majak, M. Pohlak, J. Kers, M. Saarna, G. Allikas and A. Aruniit, Design and testing of sandwich structures with different core materials, Journal of Material Science, 18(1) (2012) 45-50.

[28] AS1012.2:2014: Methods of testing concrete, Method 1: Sampling of concrete, Australian Standard, 2014.

[29] ASTM C293 / C293M-16, Standard Test Method for Flexural Strength of Concrete (Using Simple Beam With Center-Point Loading), ASTM International, West Conshohocken, PA, 2016.

[30] Standards Chinese Standard GB/T 50081-2002: Standard for test method of mechanical properties on ordinary concrete, Chinese Standard, Beijing, 2002.

[31] S. Ali, X. Liu, S. Fawzia, D. Thambiratnam, Y. Gu, and A. Remennikov, Parametric study on cement treated aggregate panel under impact load, Journal of Archives of Civil and Mechanical Engineering, 18 (2) (2018), 622-629.

[32] J. Londono, L.B. Vergiat, and H. Waisman, A Prony-series type viscoelastic solid coupled with a continuum damage law for polar ice modelling, Journal of Mechanics of Materials, 98 (3) (2016), 81-97.

[33] H.F. Brinson, and L.C. Brinson. Polymer Engineering Science and Viscoelasticity. Springer, 2008.

[34] A. Modarres, H. Shabani, Investigating the effect of aircraft impact loading on the longitudinal top-down crack propagation parameters in asphalt runway pavement using fracture mechanics, Journal of Engineering Fracture Mechanics 150 (2015), 28-46.

[35] P. Kmiecik, and M. Kaminski, Modelling of reinforced concrete structures and composite structures with concrete strength degradation taken into consideration, Journal of Civil and Mechanical engineering, 11(3) (2011), 623-636

[36] I. Jankowiak, W. Kakol, and A. Madaj, Identification of a continuous composite beam numerical model based experimental tests. 7th Conference on Composite Structures, 2005, Zielona Gora, Poland, 163-178.

[37] S. Ali, X. Liu, S. Fawzia, D. Thambiratnam, and A. Remennikov, Performance of protective concrete runway pavement under aircraft impact loading, Journal of Structure and Infrastructure Engineering, 10(4) (2020), 1-13.

[38] J. Wu, J. Liang, S. Adhikari, Dynamic response of concrete pavement structure with asphalt isolating layer under moving loads, Journal of Traffic and Transportation Engineering 1 (6) (2014) 439-447.

[39] S. Ali, X. Liu, S. Fawzia, and D. Thambiratnam, Study of the mechanical performance of the improved multi-layer composites under drop weight impact loads, International Journal of Structural Stability and Dynamics, 20(6) (2020), 1-12.

[40] Y. Huang, Pavement Analysis and Design, Prentice Hall, 1993.

[41] S. Ali, X. Liu, S. Fawzia, Numerical study on the surface depression of the concrete runway pavement under impact load, International Journal of Research in Civil Engineering, Architecture and Design, 4 (1) (2016) 8-19.

[42] G. Leonardi, Finite element analysis of airfield asphalt pavement, Archives of Civil Engineering, 60 (3) (2014) 323-334.
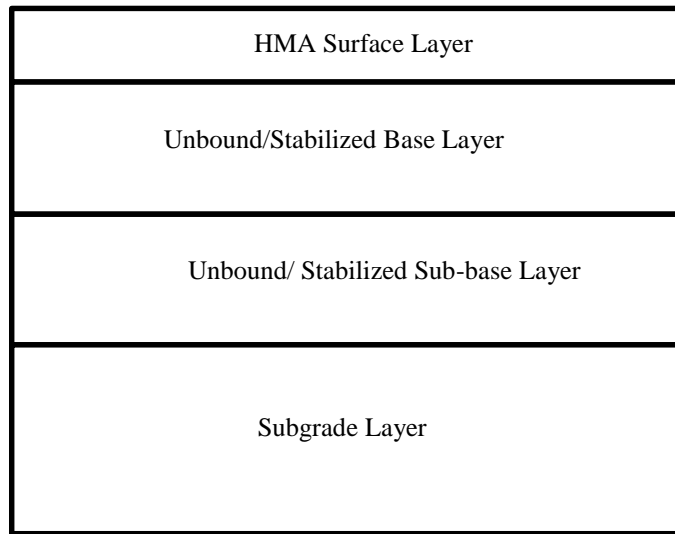
Figure 1: Composition of conventional flexible runway pavement in Australia

HMA Surface Layer

Unbound/Stabilized Base Layer

Unbound/ Stabilized Sub-base Layer

Subgrade Layer

350 mm

85 mm Asphalt Concrete
Concrete layer

265 mm Cement Treated
Aggregate layer

75 mm

Galvanized Hollow Steel Tube
Do 27 mm Di 21 mm

250 mm   500 mm   250 mm
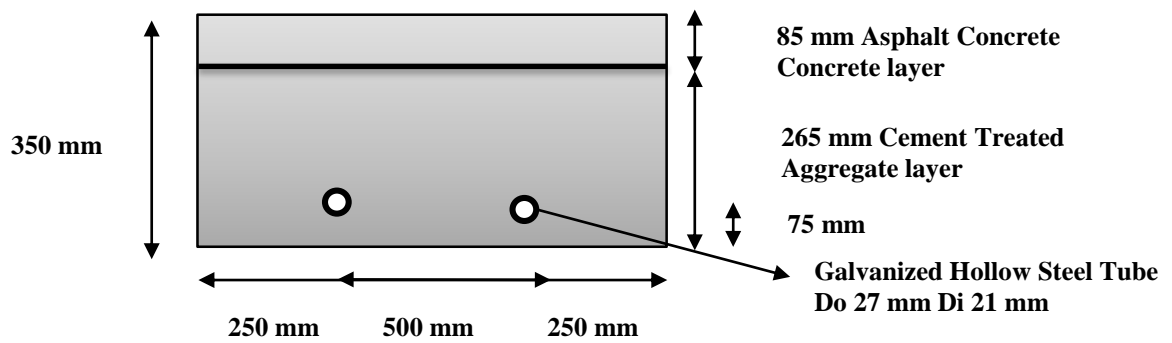
Figure 2: Composition of conventional pavement specimen

(a)

200 mm

45 mm

(b)

30 mm   580 mm   380 mm

30 mm

470 mm

500 mm

310 mm

370 mm

320 mm

C

B

Centre

A

500 mm   70 mm   430 mm
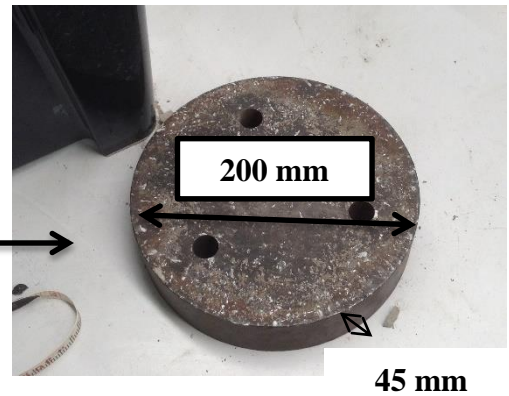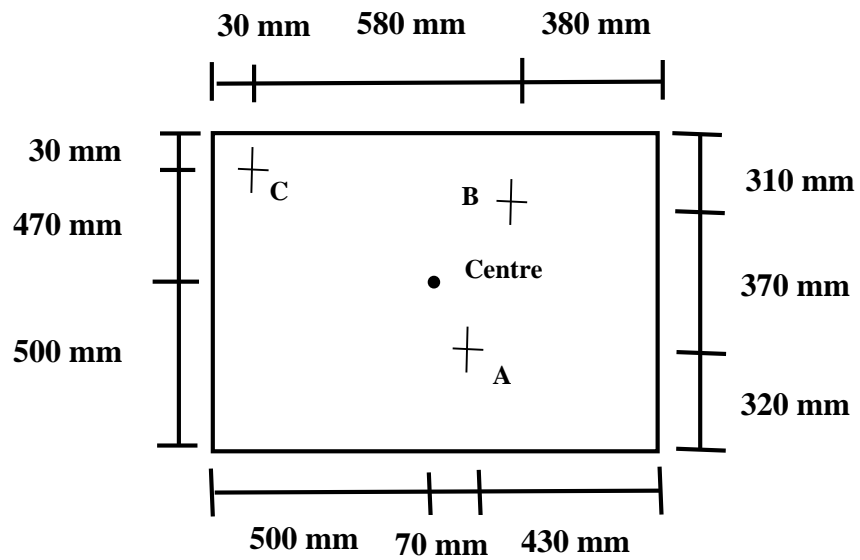
(c)

Figure 3: Test set up of composite specimen (a) test set-up (b) load distribution plate
(c) LVDT positions on top of asphalt concrete layer
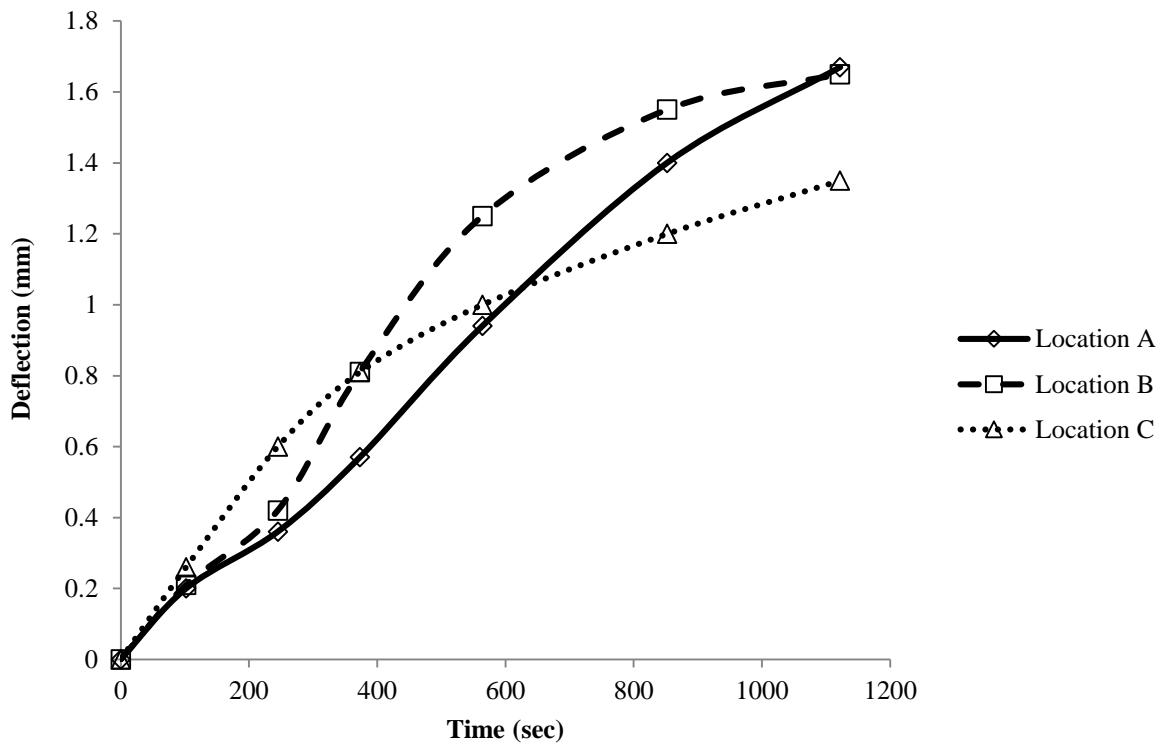
Figure 4: Deflection histories in composite specimen at different locations A, B and C
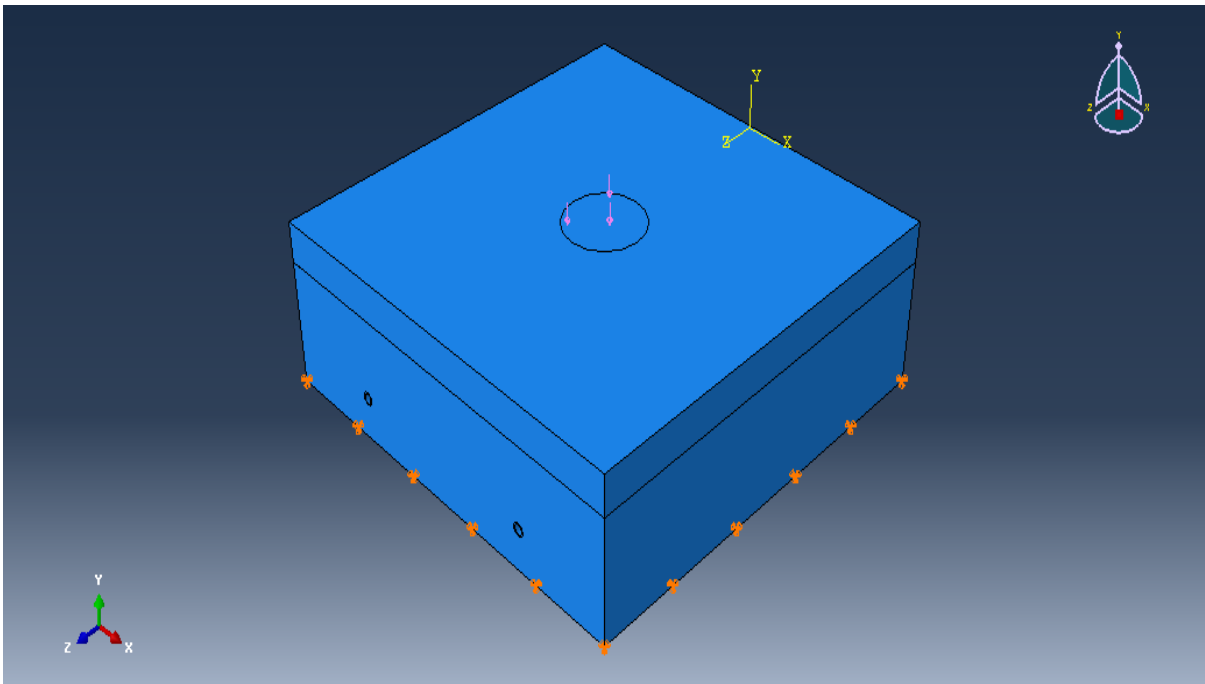
(a)
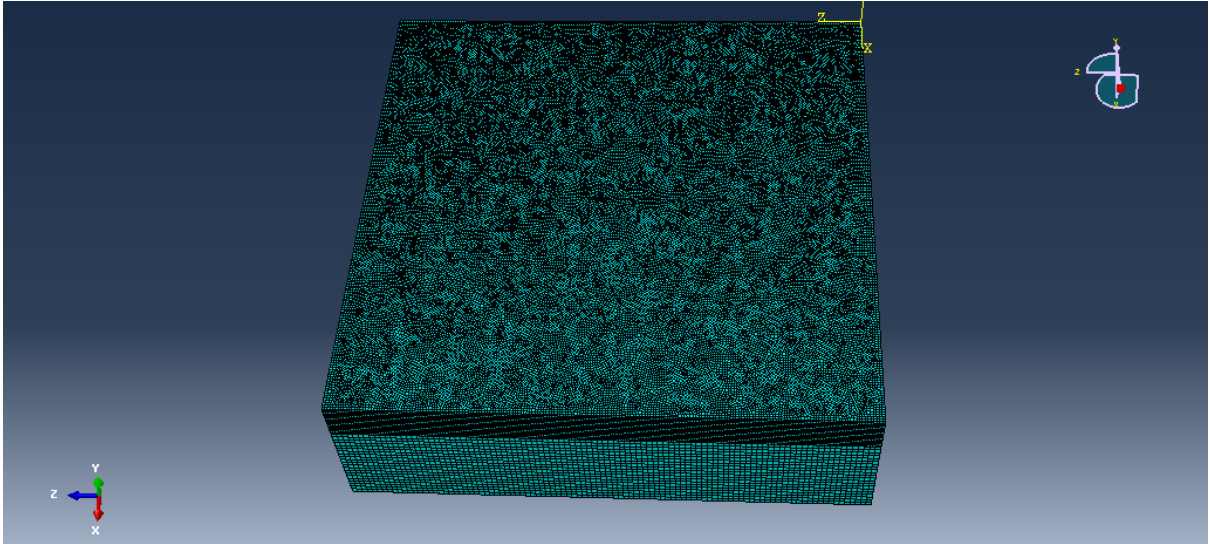
(b)

Figure 5: Finite element model of composite specimen showing (a) FE model and (b) FE mesh
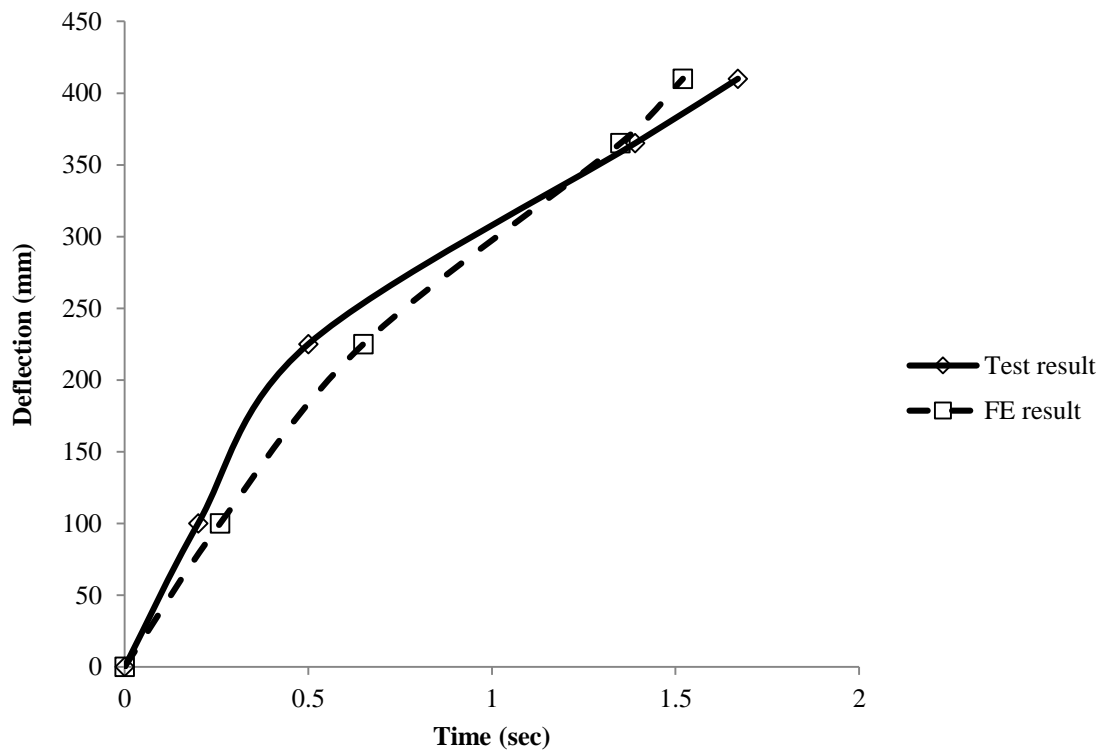
(a) Location A
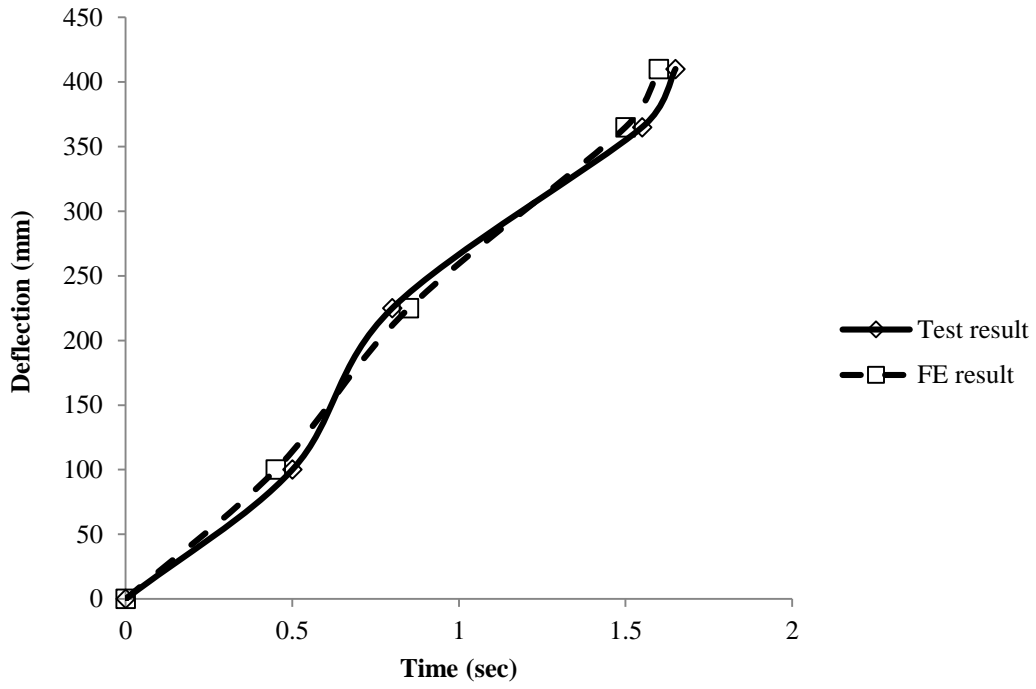
(b) Location B
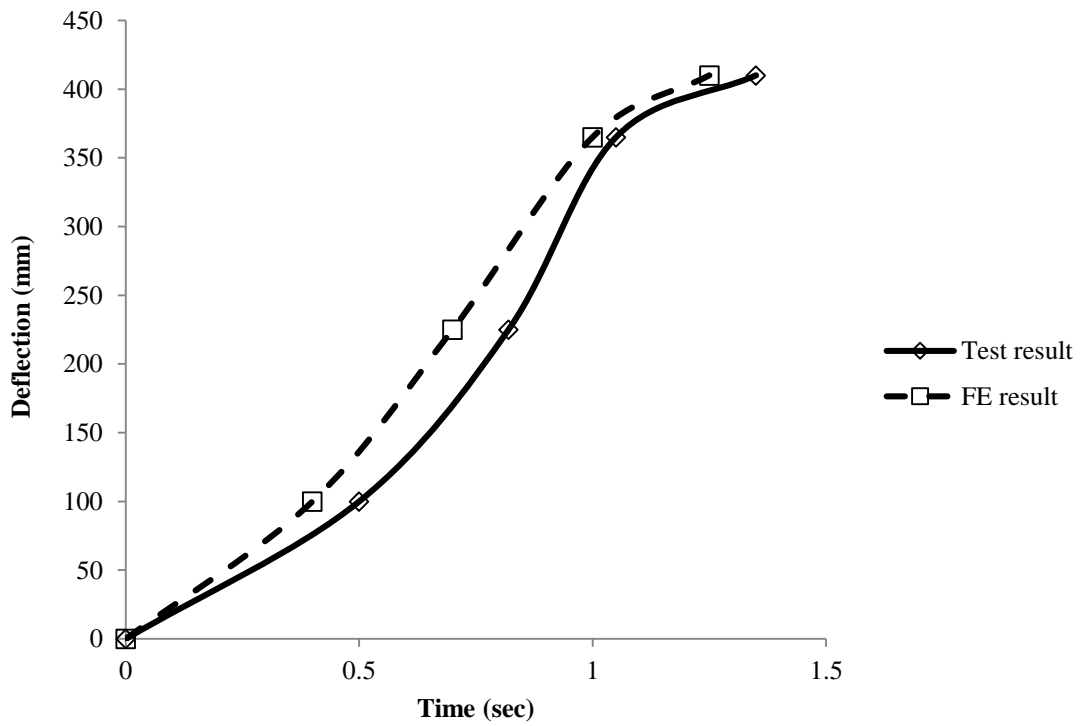
(c) Location C

Figure 6: FE and test load deflection curves at locations A, B and C of composite

specimen
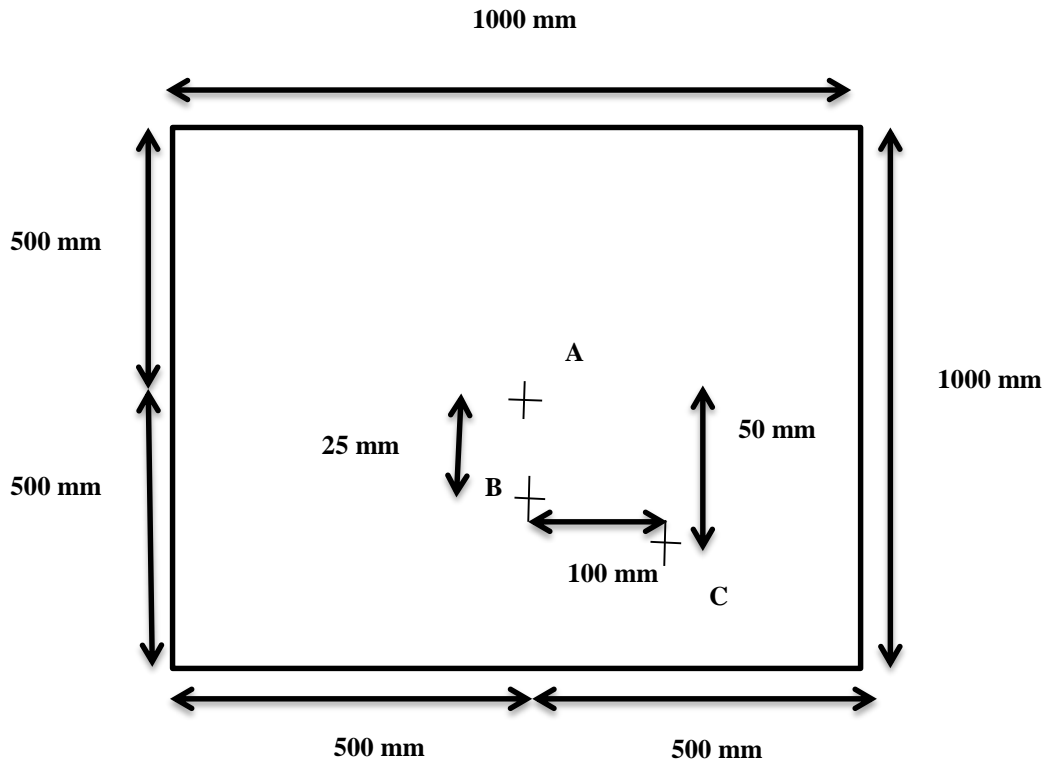
Figure 7: Measurement locations at top surface of asphalt concrete layer for feasibility

study
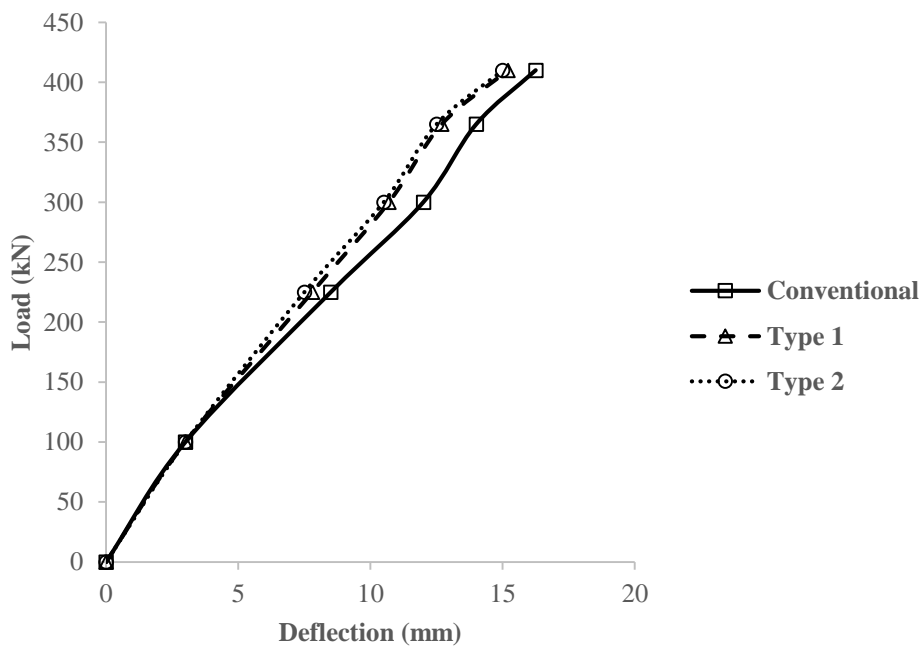
(a) Location A
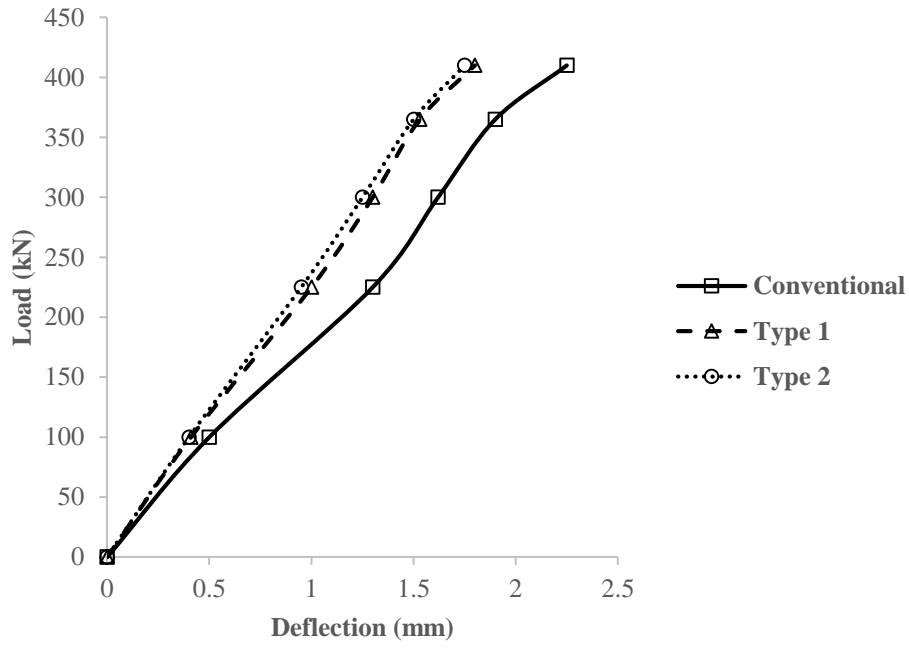
(b) Location B
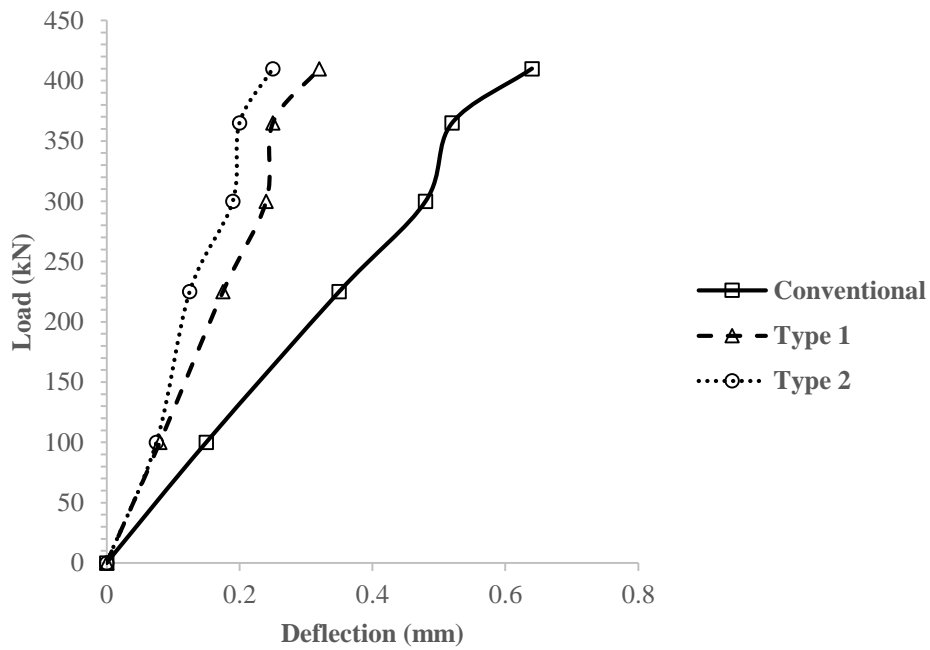
(c) Location C

Figure 8: Feasibility study of multi-layer composite specimens at locations A, B and C

7

Figure 9: Wheel tracking test carried out by Su et al. (2009)
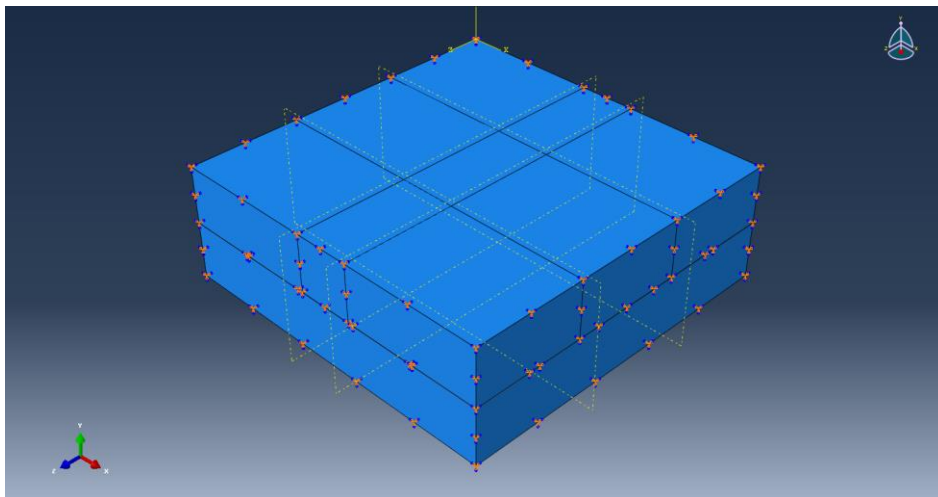
Figure 10: FE model of asphalt concrete sample with steel base
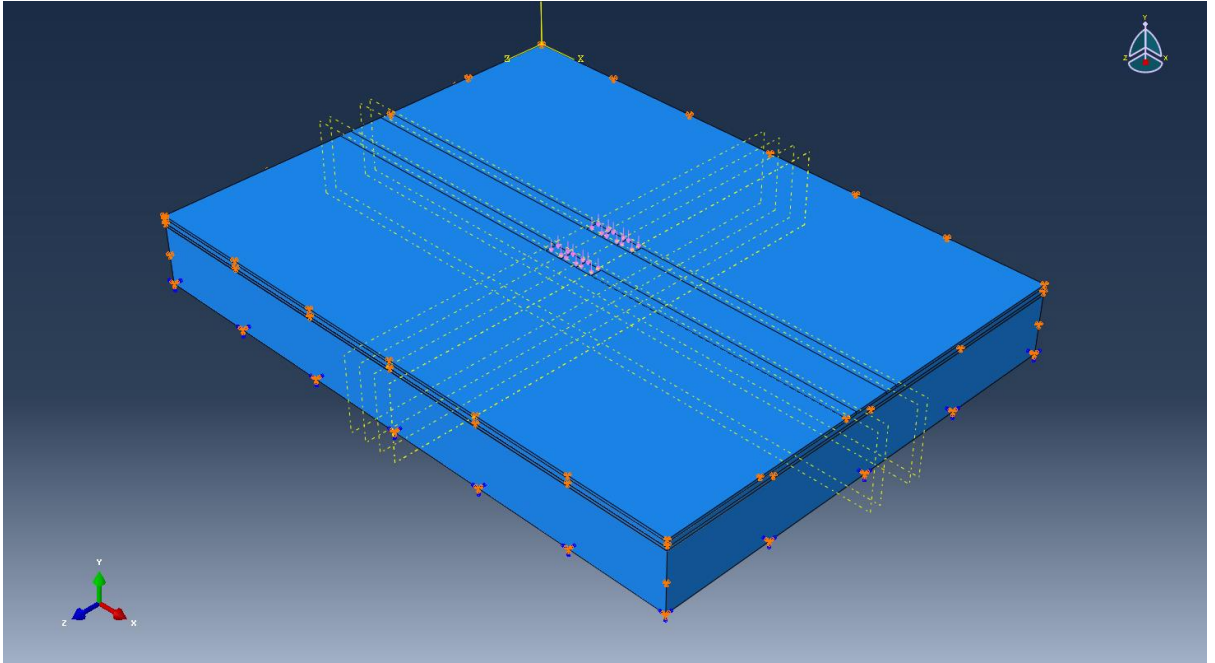
(a) FE model
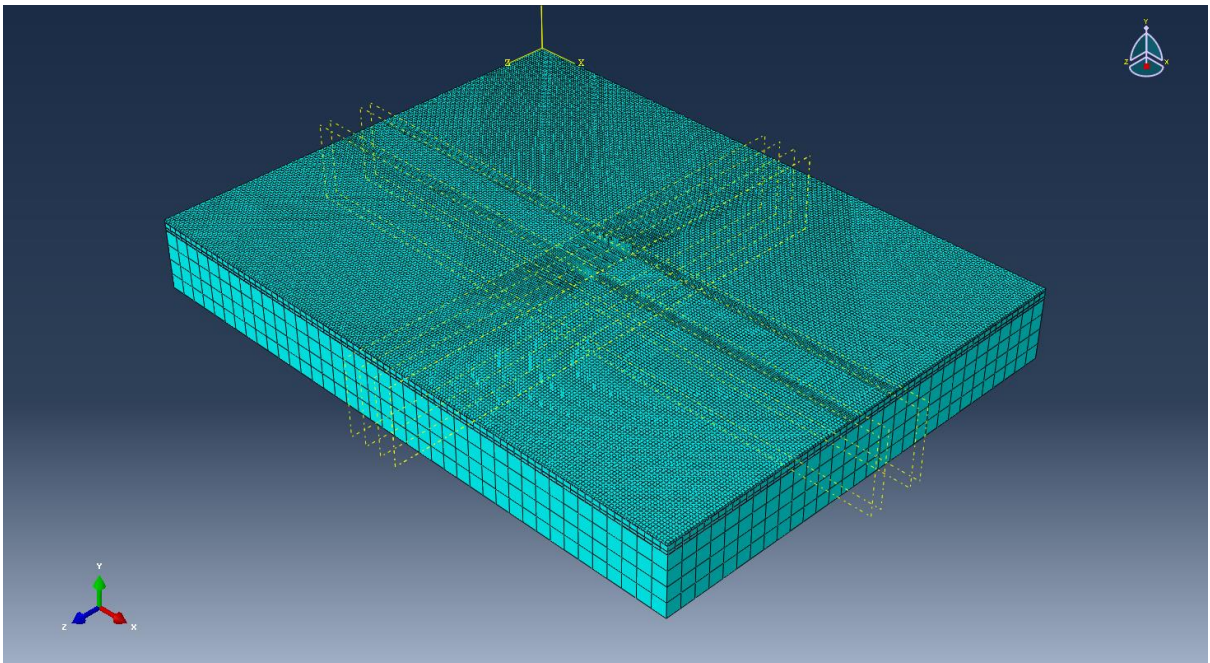
(b) FE meshing

Figure 11: FE model of composite runway flexible pavement under moving load from

aircraft (a) FE model (b) FE meshing
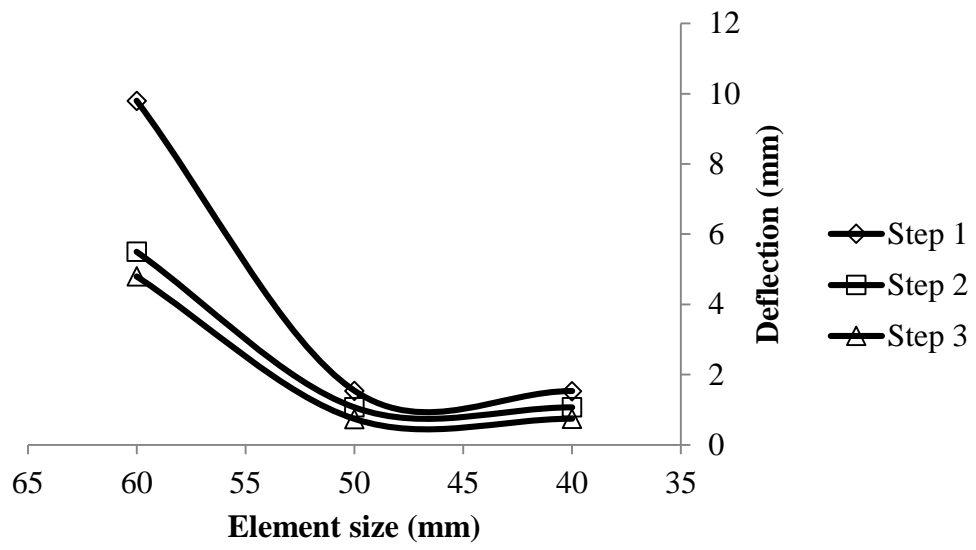
Figure 12: FE mesh convergence study
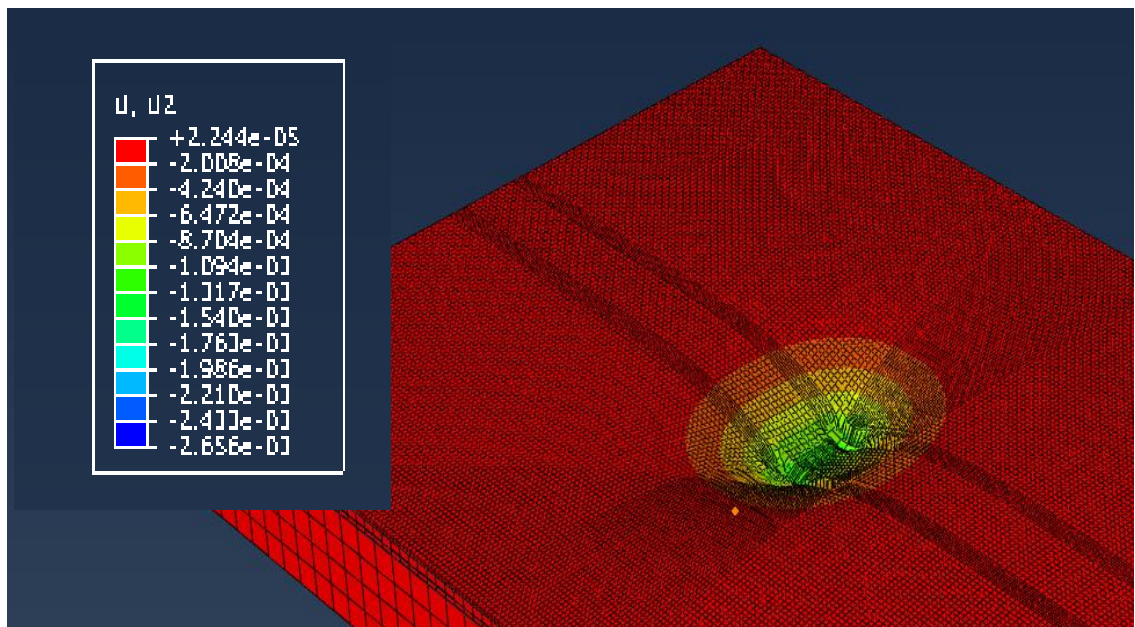
(a) Step 1(first loading zone)
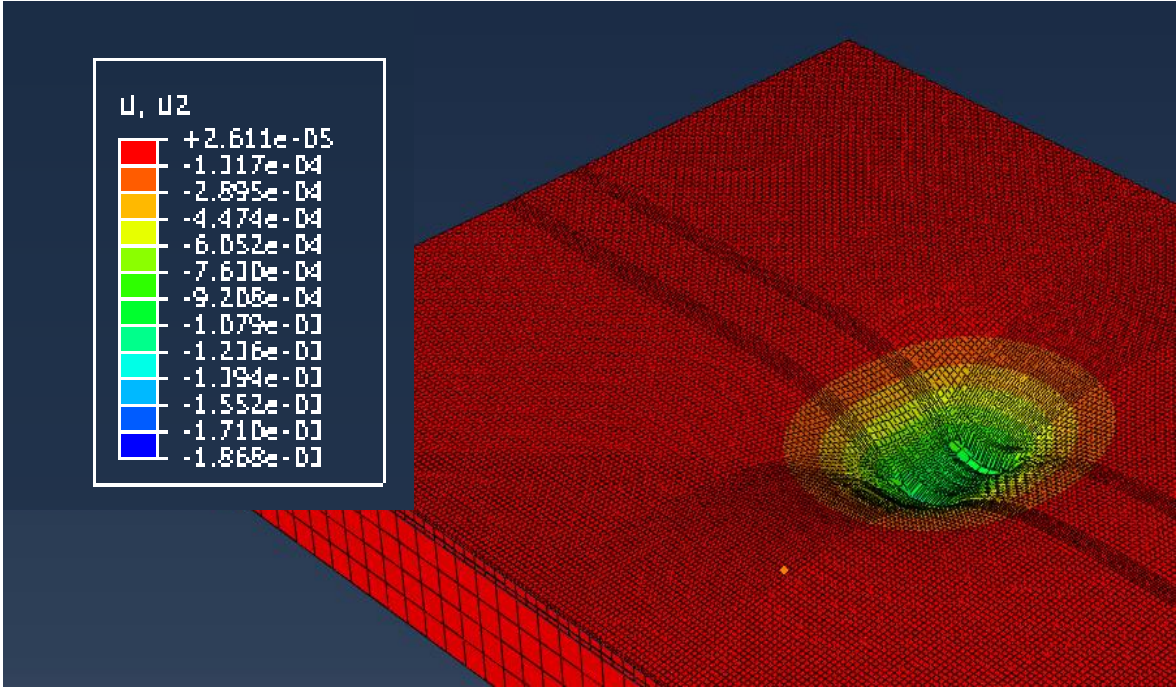
(b) Step 2 (second loading zone)
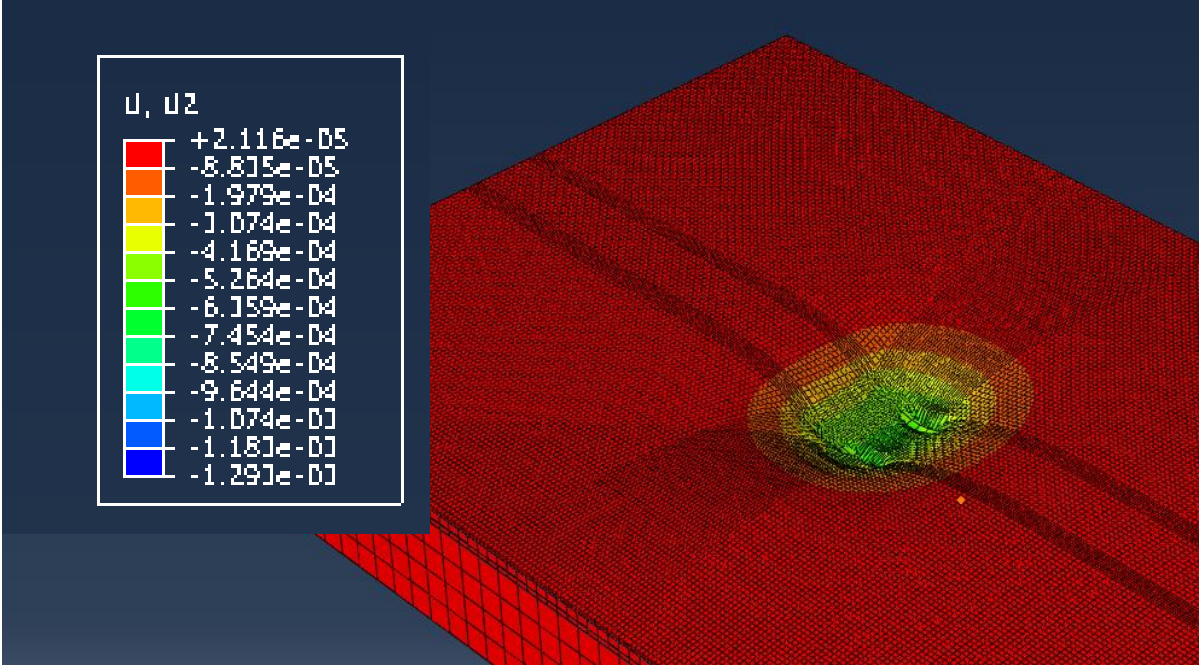
(c) Step 3(third loading zone)

Figure 13: Rut depths of proposed (Type 2) runway pavement at three loading steps (a)
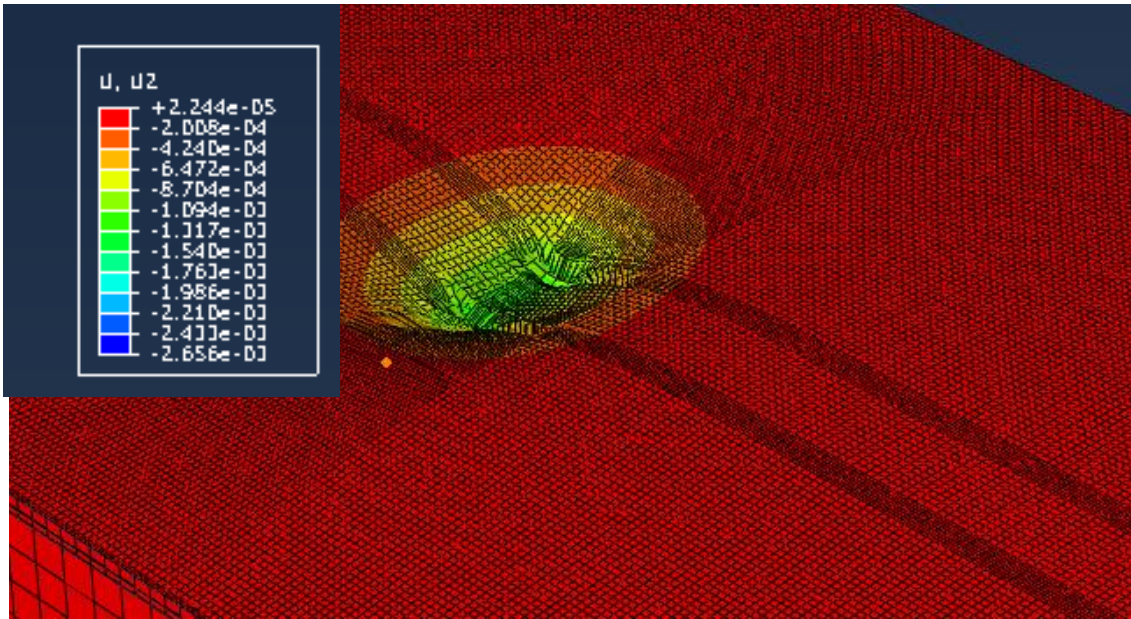
Step 1 (b) Step 2 (c) Step 3
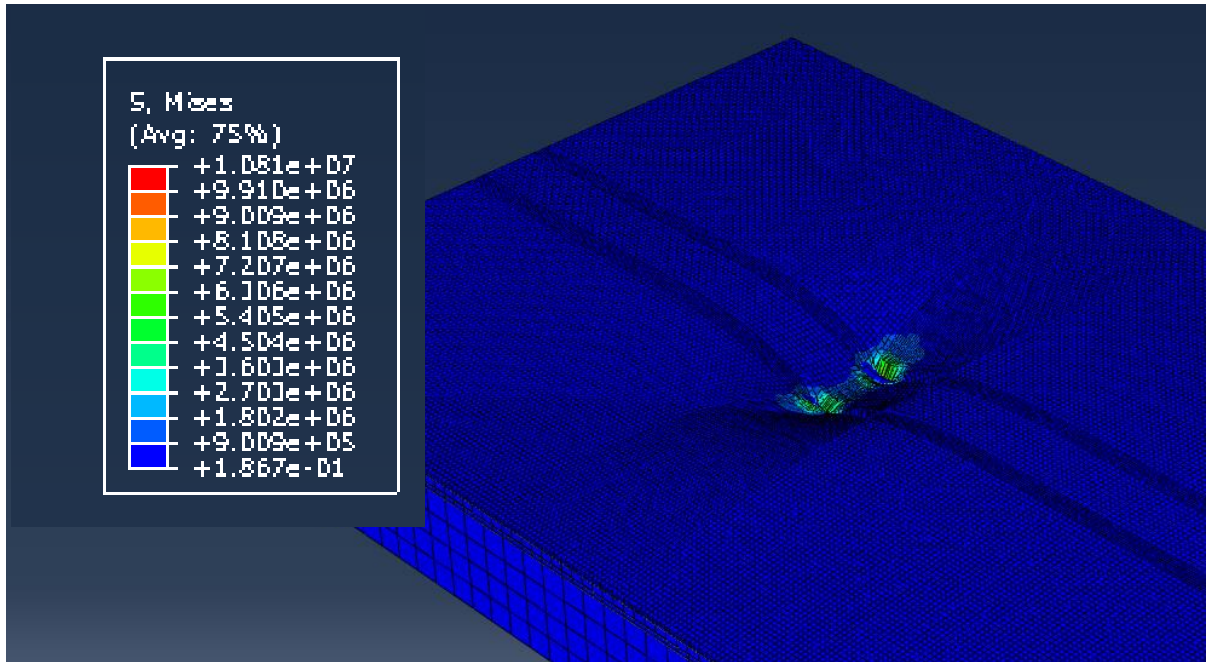
(a) Step 1(first loading zone)
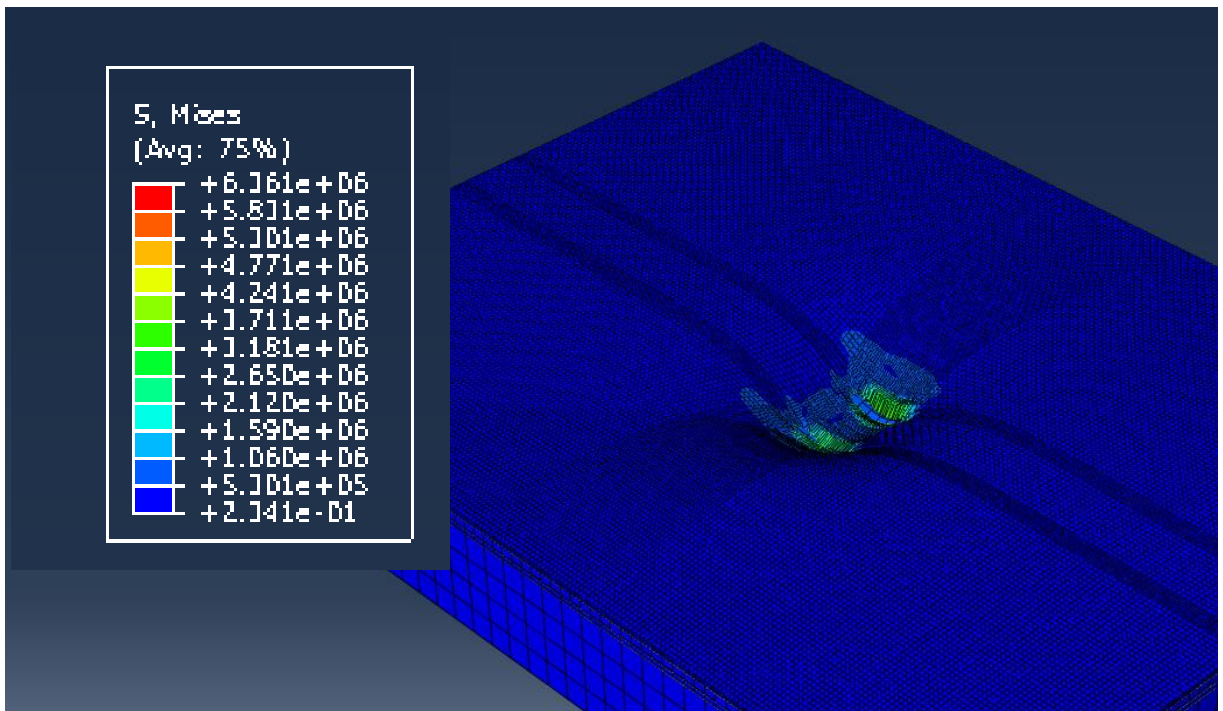
(b) Step 2 (second loading zone)
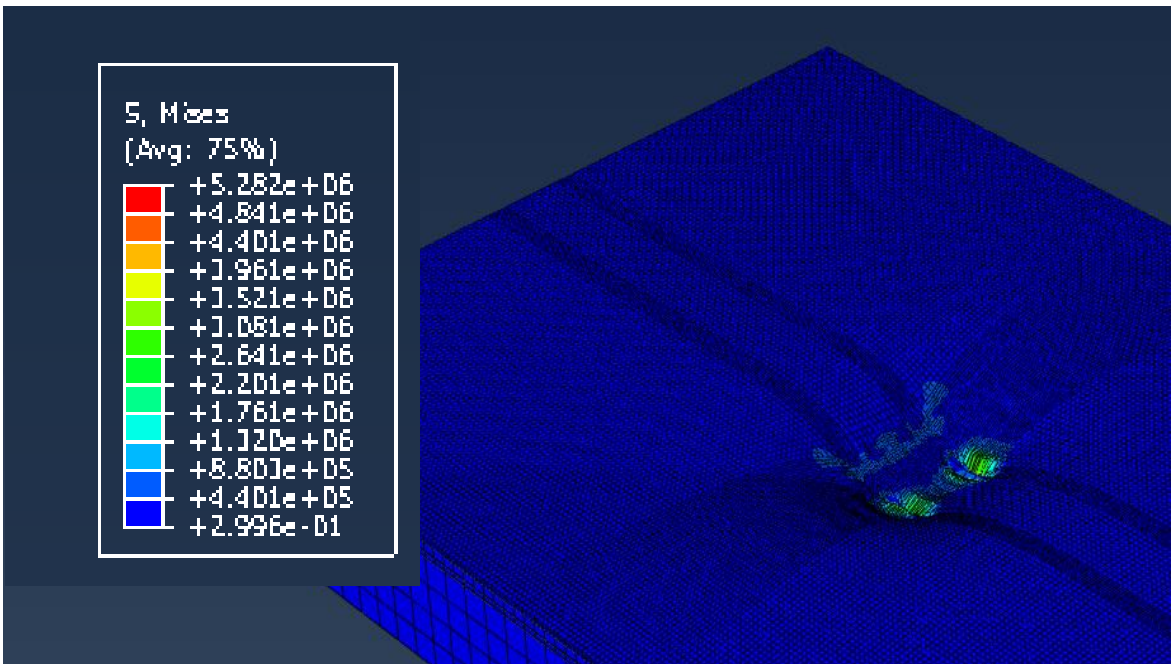
(c) Step 3 (Third loading zone)

Figure 14: Shearing resistance of proposed (Type 2) runway pavement at three loading

steps (a) Step 1 (b) Step 2 (c) Step 3

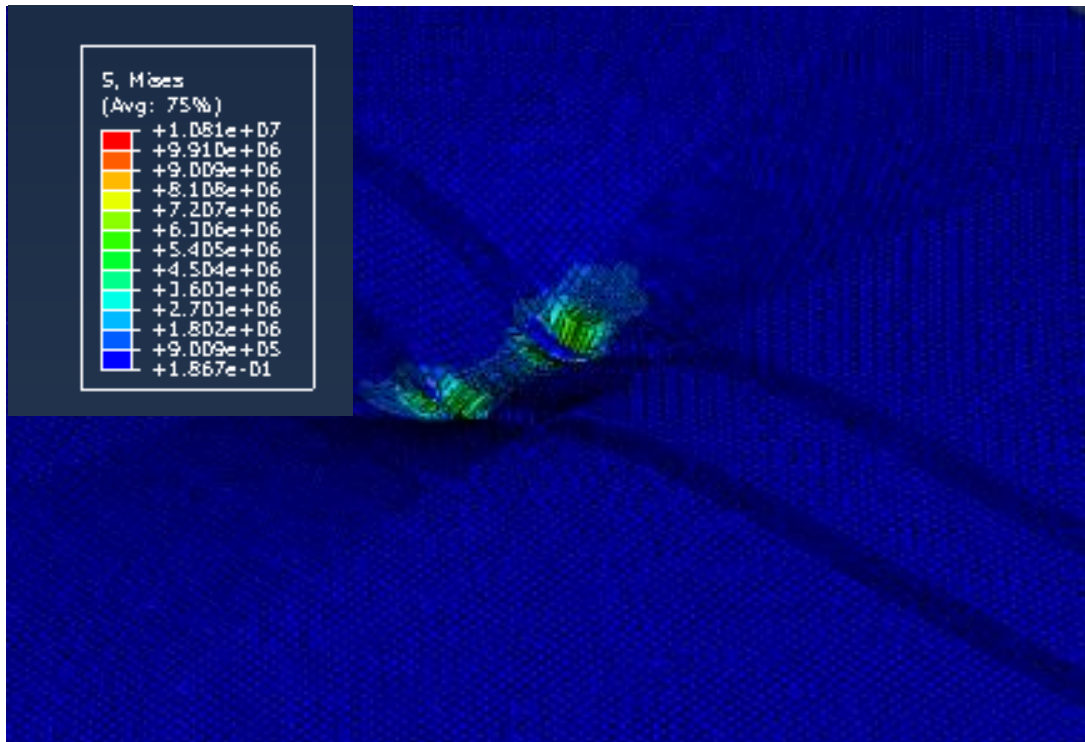Figure 15: Rut depth of proposed (Type 2) runway pavement at 50 cycles

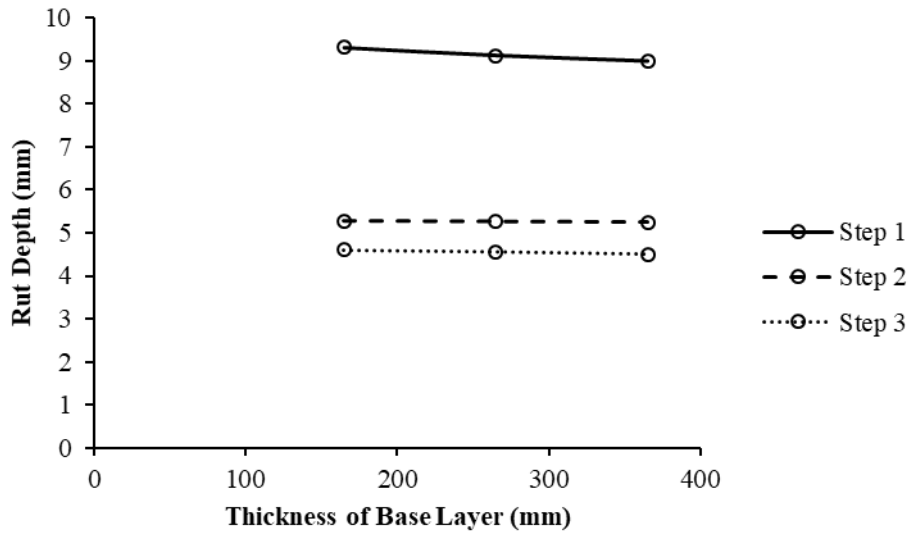Figure 16: Shearing resistance of proposed (Type 2) runway pavement at 50 cycles

Figure 17: Effect of thickness of base layer on rut depth under moving load
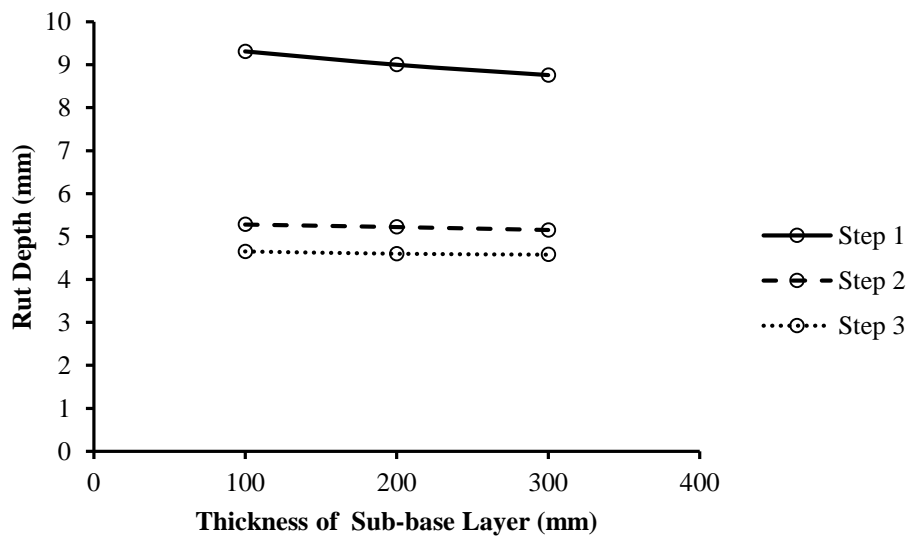

Figure 18: Effect of thickness of sub-base layer on rut depth under moving load
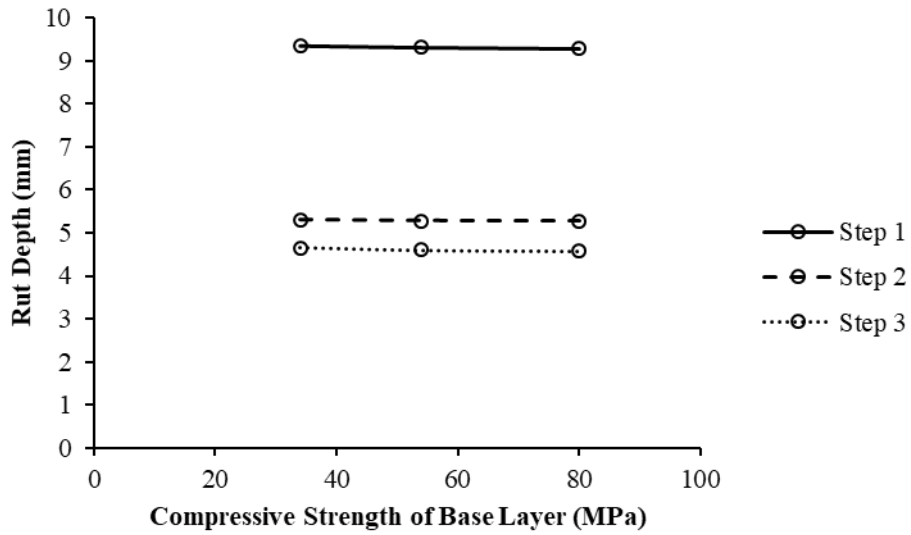
Figure 19: Effect of compressive strength of base layer on rut depth under moving load
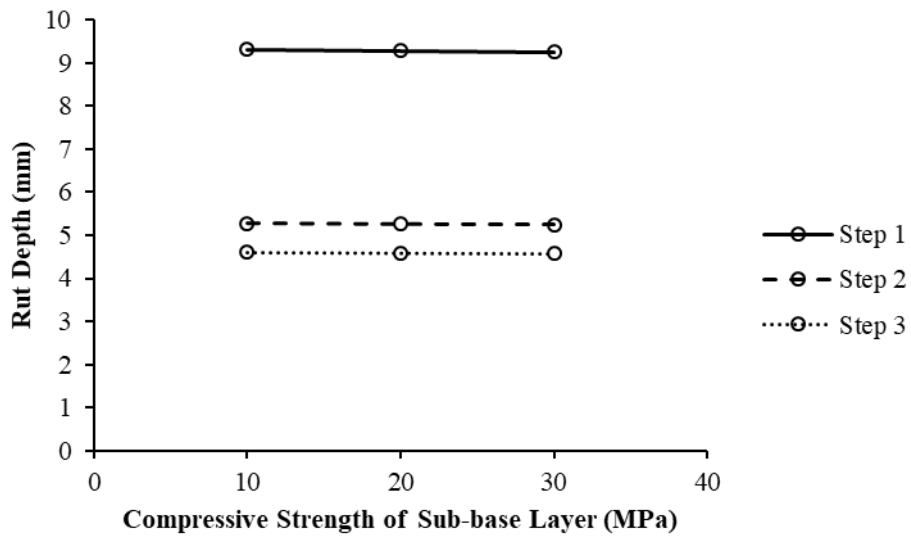

Figure 20: Effect of compressive strength of sub-base layer on rut depth under moving
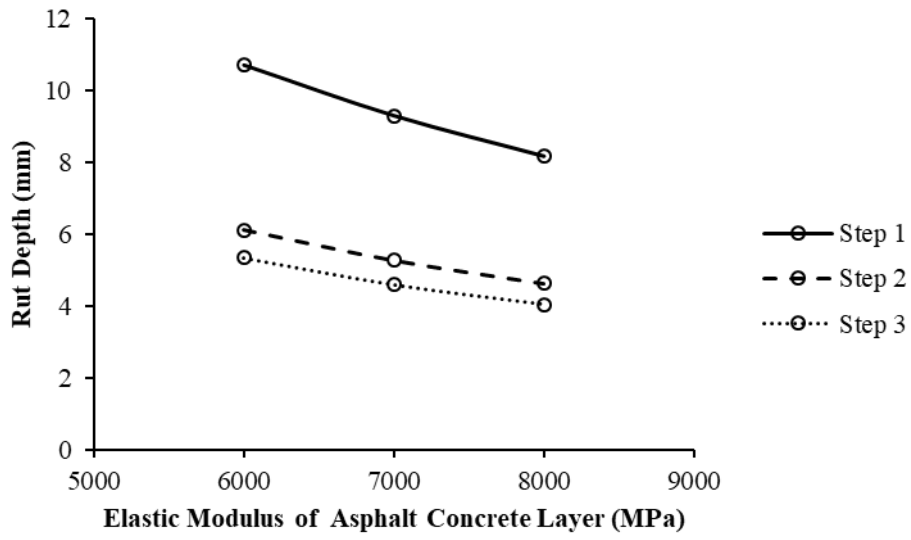
load

Figure 21: Effect of elastic modulus of asphalt concrete layer on rut depth under moving

load

Table 1 Materials and geometrics of the conventional and proposed multi-layer composite runway pavement

Composite specimen	Composite layer	Thickness (mm)	Material	Compressive strength (MPa)
Conventional	Surface layer	85	Asphalt concrete	0.15
	Base & Sub-base layer	265	Cement treated aggregate	22.5
Type 1	Surface layer	85	Asphalt concrete	0.15
	Base layer	165	High strength concrete	54
	Sub-base layer	100	Cement treated aggregate	22.5
Type 2	Surface layer	85	Asphalt concrete	0.15
	Base layer	165	High strength concrete	54
	Sub-base layer	100	Cement mortar	10

Table 2 Material properties used in FE model analysis and validation

Material	Parameters	Value
Asphalt concrete	Density (Kg/m³)	2200
	Modulus of elasticity (MPa)	60
	Poisson's ratio	0.30
Cement treated aggregate	Density (Kg/m³)	2400
	Modulus of elasticity (GPa)	1
	Poisson's ratio	0.24
	Compressive strength (MPa)	22.5
	Tensile strength (MPa)	1.40
	Dilation angle	35
	Eccentricity	0.10
	Ratio of biaxial & uniaxial strength	1.12

Table 3 Significance of proposed multi-layer composite runway pavement in reducing deflection

Location	Maximum Deflection (mm)			Maximum Deflection Ratio	
	Conventional	Type 1	Type 2	Type 1/Conventional	Type 2/Conventional
A	16.25	15.10	15.00	0.93	0.92
B	2.25	1.80	1.75	0.80	0.78
C	0.64	0.32	0.25	0.50	0.39